Induced Magnetization Density and f-d Bonding in UGe_3

G. H. Lander and J. F. Reddy
Argonne National Laboratory, Argonne, Illinois 60439

and

A. Delapalme
Laboratoire Leon Brillouin, Orme des Merisiers, F-91190 Gif-sur-Yvette, France

and

P. J. Brown
Institut Laue-Langevin, F-38042 Grenoble, France
(Received 17 December 1979)

A polarized-neutron study of the compound UGe_3 has revealed that the susceptibility at the Ge atom is paramagnetic and highly aspherical. A fit to experiment has been obtained with a single $4d_{z^2}$ orbital at the Ge site. Such an effect probably arises from charge transfer from U to Ge and strong hybridization with the unoccupied Ge $4d$ states.

One major question in the study of actinide materials is what role the $5f$ electrons play in the bonding of the solid. In metallic systems, or those with small actinide-actinide separation, considerable doubt surrounds the role of the actinide $5f$ and outer electrons in promoting bonding. Experimental tests of such concepts are often difficult to interpret uniquely because of the contribution of competing mechanisms. Examples of a system in which the actinide atoms are well separated, and thus direct $5f$-$5f$ interactions are weak, are compounds with the ordered cubic $AuCu_3$ structure, in which the nonactinide atom is from the group-III or group-IV series. Bonding in the AX_3 systems (where A is an actinide) has recently been viewed as arising from an f-d bond for transition metal X = Ir, Rh, etc., and from an f-p bond in X = Ge, Sn, Pb,... systems. In this Letter, we report the results of a polarized-neutron study of the field-induced magnetization density in UGe_3. The large positive induced magnetization density found at the Ge site is attributed to the hybridization (bonding) between the U $5f$ and $4d$ conduction electrons at the Ge site, and thus provides the first direct evidence for the importance of f-d bonding in actinide-group-IV compounds.

The compound UGe_3 (a = 4.206 Å) has a temperature-independent susceptibility of 1.3×10^{-3} emu/mole.[1] The experiment consists of placing a single crystal (0.71 g) in a 48-kOe magnetic field at 5 K and measuring the ratio $\gamma(hkl)$ of the induced magnetic scattering $M(hkl)$ to the nuclear scattering $N(hkl)$ amplitudes at a number of Bragg reflections (hkl). Such experiments on paramagnetic $3d$ and $4d$ metals[2] have been extremely useful in increasing our understanding of the modifications of the outermost-electron wave functions when the atoms are brought together to form the solid. For UGe_3 the total induced moment under these conditions is only $0.0124\mu_B$ and the ratio of magnetic to nuclear scattering amplitudes is thus $\sim10^{-3}$. Precise measurements require an intense polarized beam and we have used the $D3$ instrument at the high-flux reactor, Institut Laue-Langevin, Grenoble, France, with an incident neutron wavelength of 0.89 Å. All reflections out to $\sin\theta/\lambda = 0.5$ Å^{-1}, at which point the magnetic scattering is too small to measure, have been examined in normal-beam geometry with $\vec{H}\parallel[1\bar{1}0]$. In each case a number of equibalent reflections were measured. Small corrections are necessary for the incomplete polarization ($P_i = 0.956$) and the core diamagnetism (calculated as ~10% of the paramagnetic signal). These are discussed in more detail in our previous study[3] of URh_3. An erbium filter of sufficient thickness to remove the half-wavelength component was used throughout.

With $\gamma(hkl)$ measured, we then require $N(hkl)$ to determine $M(hkl)$. In the $AuCu_3$ structure the structure factors fall into two groups:

(1) For h,k,l all even or odd (primary reflections),

$$N_+ = b_U \exp(-W_U) + 3b_{Ge} \exp(-W_{Ge}), \quad (1)$$

where b_U and b_{Ge} are the coherent scattering amplitudes of uranium and germanium, 0.852×10^{-12} and 0.819×10^{-12} cm, respectively; the Debye-Waller factors are represented by e^{-W}, where $W = B(\sin\theta/\lambda)^2$.

(2) For h,k,l with mixed indices (superlattice

reflections),

$$N_{-} = b_U \exp(-W_U) - b_{Ge} \exp(-W_{Ge}). \quad (2)$$

Similarly, for the magnetic structure factor M we may substitute p_i for b_i, where $p_i = 0.27 \times 10^{-12} \mu_i f_i(\vec{k})$ cm. The magnetic moment located at site i is given by μ_i and its spatial distribution is given by the Fourier transform of the magnetization density, $f_i(\vec{k})$, where $\vec{k}$ is the scattering vector $|\vec{k}| = 4\pi \sin\theta/\lambda$. The intensities of superlattice reflections in UGe_3 are $\sim 10^{-4}$ of the primary reflections because of the cancellation of the scattering amplitude $b_U - b_{Ge}$. With unpolarized neutrons and a conventional four-circle diffractometer, we have measured the intensities of the reflections as a function of temperature and performed a crystallographic least-squares refinement to determine the best values of the extinction, scattering lengths, and thermal parameters. This is particularly important as the uranium and germanium atoms have slightly different Debye-Waller factors. Moreover, the germanium atom has tetragonal point-group symmetry (D_{4h}), so that it is permitted to have an anisotropic thermal parameter. However, the polarized-beam experiment is at low temperature and is concerned only with reflections at low values of $\sin\theta/\lambda$ so these effects are minimized, and any uncertainties are less than the error bars shown on the superlattice reflections. Corrections for extinction on the primary reflections amount to a maximum of 15%.

The results, presented in terms of the quantity $(\mu f)_{hkl}$ are shown in Fig. 1. The most striking feature of this figure is that the μf values for the primary and superlattice reflections do not lie on one general curve, but that the former lie systematically above the latter out to $\sin\theta/\lambda = 0.4$ Å^{-1}. Inspection of Eqs. (1) and (2) shows that this can arise only if $\mu_{Ge} > 0$. Recall that we are measuring the susceptibility throughout the unit cell, not an ordered moment. Elemental germanium is *diamagnetic* and no paramagnetic susceptibility has previously been observed at a germanium site. The primary reflections in Fig. 1 represent the total susceptibility and appear to extrapolate to $\sim 12 \times 10^{-3} \mu_B$ at $\sin\theta/\lambda = 0$, in agreement with the bulk measurements denoted by the arrow in the figure. By performing a Fourier transform we can obtain the induced magnetization density and a three-dimensional view of this is given in Fig. 2. Note first the almost spherical and dominant density at the U site. We attribute this to 5*f* electrons with an attendant orbital moment since for spin only scattering[4] the amplitude would be zero at $\sin\theta/\lambda \sim 0.4$ Å^{-1}. Second, the Fourier transform shows very elegantly the highly aspherical distribution associated with the Ge

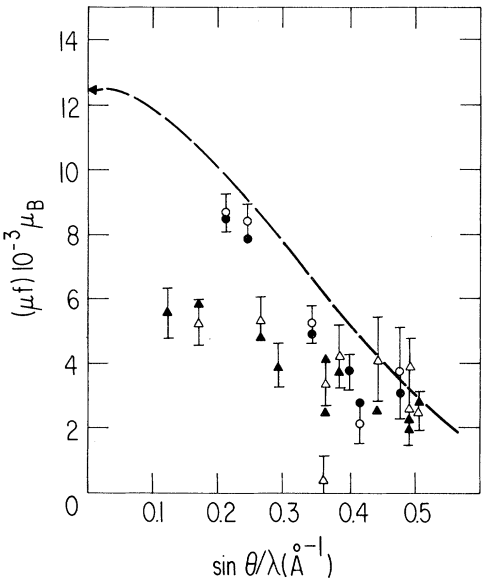

FIG. 1. Induced moment as a function of angle for UGe_3. The dashed curve would be the form factor if all the moment was located at the uranium site. The ordinate intercept is given by the static susceptibility corrected for the diamagnetic contribution. The open points are the experimental observations and the closed points are the best fit discussed in the text. Circles are primary reflections; triangles are superlattice reflections.

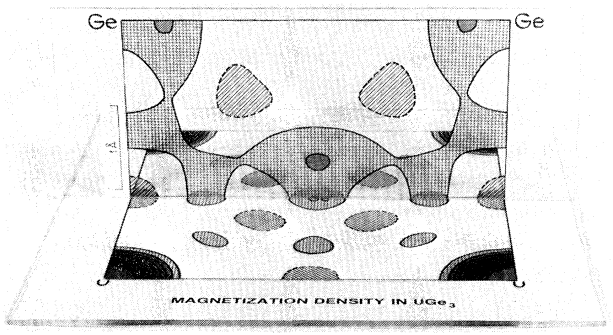

FIG. 2. Three-dimensional picture of the magnetization density in UGe_3. The base plane is a (001) plane showing a network of 4 U atoms. The Ge atom positions at $(\frac{1}{2}\,\frac{1}{2}\,0)$, $(0\,\frac{1}{2}\,\frac{1}{2})$, and $(1\,\frac{1}{2}\,\frac{1}{2})$ are shown. The hatched areas are positive density, the full areas being second contours (or > 2 at the U site), and the dashed areas are negative regions. The contour levels are at intervals of $10^{-3}\mu_B/\text{Å}^3$ with the first contour at $-0.5 \times 10^{-3}\mu_B/\text{Å}^3$.

site, which we previously inferred from Fig. 1.

To gain a more quantitative understanding of these measurements we have attempted a number of fits to the data of Fig. 1. For the uranium site we choose a localized wave function and the dipole approximation[4] so that

$$p_U = 0.27\times10^{-12}\mu_U[\langle j_0\rangle + 1.75\langle j_2\rangle] \text{ cm}. \quad (3)$$

The moment at the uranium site is μ_U, $\langle j_i(k)\rangle = \int_0^\infty \rho^2(r) j_i(kr)\, dr$, where $\rho(r)$ is the amplitude of the radial wave function, and $j_i(kr)$ are spherical Bessel functions.[4] We have chosen a $5f^3$ configuration for the uranium site but cannot distinguish between this and a $5f^2$ configuration.[4] For the Ge site we first considered scattering from a $4p$ wave function. However, as shown in Fig. 3, the $4p$ radial charge density has its maximum density at ~1.2 Å from the nucleus, whereas the maximum density associated with the Ge site appears at ~0.5 Å from the nucleus (see Fig. 2). We are in fact unable to fit the data with *any* tabulated $4p$ wave function. The next logical step is to assume, because of hybridization, that the wave function has a predominant $4d$ character. In our previous study[3] of URh_3 we found a strongly enhanced $4d$ magnetization at the Rh site, which we argued was a consequence of hybridization. Of course, the $4d$ band is already partly occupied in Rh, so that a similar experimental result in UGe_3 is more striking. In terms of susceptibility, the local value at the Ge site is $+0.11\times10^{-3}$ emu, whereas elemental Ge has a diamagnetic susceptibility of -0.03×10^{-3} emu. The scattering from a single d_{z^2} orbital (note that the Ge local site symmetry is tetragonal) is then

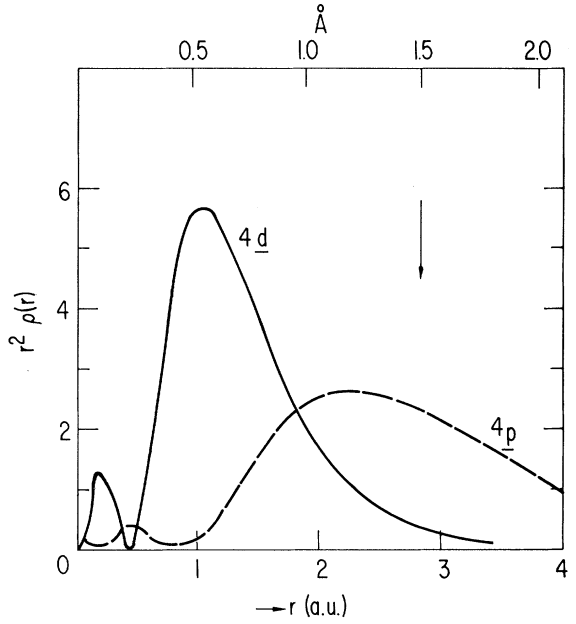

FIG. 3. Radial charge density as a function of distance from the nucleus as given by Ref. 5. The $4p$ function is from Ge; the $4d$ function is from a nearly filled $4d$ shell and is found to give the best fit to the data in Fig. 1. The vertical arrow marks half the U-Ge distance.

$$p_{Ge} = 0.27\times10^{-12}\,\mu_{Ge}(4\pi)^{1/2}\{Y_0^0\langle j_0\rangle + [(20)^{1/2}/7]\,Y_0^2\langle j_2\rangle + \tfrac{6}{7}Y_0^4\langle j_4\rangle\} \text{ cm},$$

where Y_m^l are the usual spherical harmonics. For a spherical d distribution, the terms in $\langle j_2\rangle$ and $\langle j_4\rangle$ are omitted. We have tried a series of free-atom $4d$ wave functions,[5] the best fits ($\chi^2 = 1.2$) being with a tightly compacted $4d$ function as shown in Fig. 3. The agreement with a d_{z^2} orbital is appreciably better than with a spherical distribution, as one would expect from Fig. 2. The final calculated values with $\mu_U = (7.7\pm0.4)\times10^{-3}\mu_B$ and $\mu_{Ge} = (1.6\pm0.4)\times10^{-3}\mu_B$ are given in Fig. 1. The overall agreement is remarkably good.

Band calculations have been performed on UGe_3 which compare reasonably well with de Haas–van Alphen measurements.[1] The authors point out the need for a charge transfer from U to Ge and our results are consistent with such an interpretation. With use of the potential of Ref. 1, the densities of the $l = 1$ and 2 components have been calculated[6] from the wave function at the Fermi energy and compared with those drawn in Fig. 3; the p ($l = 1$) component matches very well the atomic function, but the d ($l = 2$) component is essentially delocalized and does not resemble the $4d$ wave function in Fig. 3. A simple spin density induced from the calculated radial density will not therefore reproduce the experimental situation.

In conclusion, our measurements provide an excellent example of the dichotomy existing in actinide research. On the one hand, we find an almost totally localized spherical moment (plus orbital part) at the uranium site. On the other hand, the strong hybridization of the remaining uranium wave functions with those at the Ge site has led to the appearance of a positive, induced magnetization density at the Ge site. Because of the nature of the neutron magnetic interaction, we have been able to identify both the angular and spatial extent of this density at the Ge site. We

suggest that this effect arises from the interaction of the U 5*f* electrons with the normally unoccupied Ge 4*d* states.

We are grateful to F. Tasset for experimental assistance and to A. J. Arko, M. Brooks, A. J. Freeman, and D. D. Koelling for discussions and comments on the manuscript. This work was supported in part by the U. S. Department of Energy.

[1]A. J. Arko and D. D. Koelling, Phys. Rev. B 17, 3104 (1978).

[2]For a review, see R. M. Moon, W. C. Koehler, and J. W. Cable, in *Proceedings of the Conference on Neutron Scattering, Gatlinburg, Tennessee, 1976*, edited by R. M. Moon, CONF-760601 (National Technical Information Service, Springfield, Va., 1976), Vol. II, p. 577.

[3]A. Delapalme, G. H. Lander, and P. J. Brown, J. Phys. C 11, 1441 (1978).

[4]A. J. Freeman, J. P. Desclaux, G. H. Lander, and J. Faber, Phys. Rev. B 13, 1168 (1976).

[5]E. Clementi and C. Roetti, At. Data Nucl. Data Tables 14, 177 (1974).

[6]D. D. Koelling, private communication.

Electron and Hole Capture at Au and Pt Centers in Silicon

S. D. Brotherton and J. E. Lowther[a]

Philips Research Laboratories, Redhill, Surry RH1 5HA, United Kingdom

(Received 11 December 1979)

Emission rates and hole-capture cross sections for the Au donor center in silicon are reported and from entropy considerations this center is shown to be similar in behavior to the Pt donor center. In contrast, the gold and platinum acceptor states display significantly different entropy changes on electron emission. A similar chemical structure for both these defects is proposed which is then used to interpret differences in electron emission behavior from the acceptor forms of the two defects.

Present understanding of carrier recombination at deep defects in silicon is not at all complete. Not only is there lack of fundamental knowledge concerning carrier recombination at the defect but, particularly for many technologically important defects, any real theoretical progress has been hindered because of the absence of a detailed understanding of the chemical nature of the defect concerned. Mott[1] has recently reviewed mechanisms of carrier recombination and noted that this process usually involves a lattice relaxation—the physical significance of which depends upon the strength of the electron-lattice coupling at the center and therefore the structural form of the defect in the lattice.

In this work, we report emission rates and hole-capture cross sections for the Au donor. These measurements complement those reported earlier.[2,3] We then compare the electrical properties of Au and Pt centers in the light of a structural model which we associate with both defects.

In previous publications[2,3] the electrical characterization of the gold acceptor level and the platinum donor and acceptor levels in silicon were presented. The measurements on the gold donor level, necessary to complete the comparison between gold and platinum centers in silicon, are described below.

The hole-emission and -capture rate measurements on the gold donor level were made at constant capacitance using gated n^+p diodes which had been gold diffused. A typical deep-level transient spectroscopy (DLTS) spectrum obtained from such a diode is shown in Fig. 1; peak *A* is the gold donor level and peak *B* is due to the small relaxation in occupancy taking place at the gold acceptor level. Thermal activation

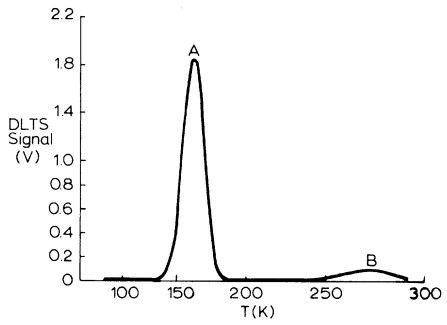

FIG. 1. DLTS trace obtained from a gold-doped n^+p diode ($\tau = 14.2$ ms).

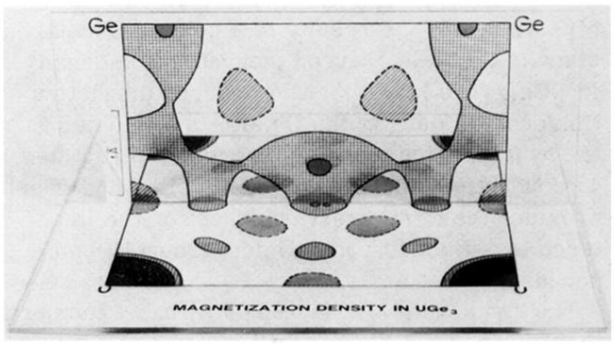

FIG. 2. Three-dimensional picture of the magnetization density in UGe_3. The base plane is a (001) plane showing a network of 4 U atoms. The Ge atom positions at $(\frac{1}{2}\,\frac{1}{2}\,0)$, $(0\,\frac{1}{2}\,\frac{1}{2})$, and $(1\,\frac{1}{2}\,\frac{1}{2})$ are shown. The hatched areas are positive density, the full areas being second contours (or > 2 at the U site), and the dashed areas are negative regions. The contour levels are at intervals of $10^{-3}\mu_B/\text{Å}^3$ with the first contour at $-0.5\times 10^{-3}\mu_B/\text{Å}^3$.